CALIBRATION AND OPERATION OF A POSITIONING ROBOT USED FOR MINIMALLY INVASIVE VASCULAR INTERVENTIONAL SURGERY

XUE YANG[1], HONGBO WANG[2], ZHEN XU[1], HONGNIAN YU[2], ZENGGUANG HOU[3]

Abstract. This paper presents the calibration and operation modes of a positioning robot used for minimally invasive vascular interventional surgery. Firstly, the constitution of positioning robot, the calibration method using an absolute encoder and the operation method using a six-dimensional force sensor are described. Then, the operation mode is proposed based on a six-dimensional force sensor, which includes the force signal transform of the six-dimensional force sensor, the calculation method of the end position of the positioning robot obtained by the six-dimensional force sensor, and the inverse kinematics of the positioning robot. Finally, the experiment is conducted and the experimental results demonstrate the proposed method is effective, safe, and reliable and has a potential application, which provides a good supporting case for the HAM framework.

Key words: surgery robot, minimally invasive, calibration, operation, six-dimensional force sensor.

1. INTRODUCTION

A surgery robot is used for patients and its security is a vital indicator for system evaluation. So an intelligent surgery robot should be a human adaptive mechatronics (HAM) system. The HAM main aim is to introduce a capability that the machine can measure or understand the level of the skills of its human operator to a human-machine system [1]. The key idea of HAM is to develop a system which includes the human in the control loop and changes the functions and structure of the man-machine interface to improve the machine's controllability.

Research on surgical robotics has been received intensive attention recently. The new research direction may lead to the development of very different robotic surgical devices in the future. Minimally invasive surgical techniques rose in the 1980s, whose character is to achieve a minimally trauma therapeutic. Minimally invasive vascular interventional surgery is one of the minimally invasive surgeries. Vascular interventional surgical is the Digital Subtraction Angiography (DSA) to guide the doctor to insert the catheter into blood vessels and cure lesions so that the

---

[1] College of Mechanical Engineering, Yanshan University, CN.
[2] Staffordshire University, UK.
[3] Institute of Automation, Chinese Academy of Sciences, CN.

catheter reaches the embolism and malformed vascular to dissolve the clot of narrow blood vessels or to use other purposes [2, 3]. Minimally invasive surgery has the advantage of minimally invasive, early recovery and painless, and rapidly becomes the development trend of the modern surgery [4]. However, due to the limitations of manual surgical intervention, the development of a minimally invasive vascular interventional surgical robot is required. Therefore, the robot technology applied to the surgical system has the following advantages: more accurate device selection, better visualization, shorter procedure duration, less contrast media and reduces radiation exposure [5–8]. Robotic systems have been suggested to enhance the precision of cardiovascular procedures with increased accuracy [9–15].

The world's first surgical robot was the "Arthrobot" [16] which was developed and used for the first time, in Vancouver BC, Canada in 1983. In 1985, a robot PUMA 560 was used to place a needle for a brain biopsy using the CT guidance [17]. In 1988, the PROBOT, developed by Imperial College London, was used to perform the prostatic surgery [18]. The ROBODOC from Integrated Surgical Systems was introduced in 1992 to mill out precise fittings in the femur for hip replacement [19]. Further development of robotic systems was carried out by Intuitive Surgical with the introduction of the Davinci Surgical System and Computer Motion with the AESOP and the ZEUS robotic surgical system [20, 21]. German Aerospace Center (DLR) showed how the entry point (trocar) can be estimated, followed by the calculation of the inverse kinematics [22]. University of Paris 12 proposed and developed an active catheter with a multi micro-robots stack arranged inside its external sheath [23]. Korea Advanced Institute of Science and Technology suggested a human arm-liked robotic surgical system for laparoscopic surgery [24, 25]. According to Intuitive Surgical requirements, 205,000 Davinci assisted procedures were performed in 2009, up 51% from 2008 [26]. Recently, minimally invasive surgery robots were used on hepatic resection [27], partial nephrectomy [28] and hypopharyngeal carcinoma [29] operations.

Robots need to calibrate its original position before operating. The calibration with a large range of movement needs a little more time and a certain space, which will influence the efficiency and limit the application environment of the robot. In addition, the robot operation is mainly relying on the given procedure by programming, and the operator could not operate the robot discretionarily.

Although the surgical robotics research is booming, but most of the systems are being studied in the labs environment, and the systems used in clinical practice are few. This paper proposes a new reposition and operation mode for a minimally invasive surgery robot to save calibration time and accomplish compliance control of the robot. The robot introduced in this paper is operated by operator through a six-dimensional force sensor which is used to identify human behavior and operation.

2. CALIBRATION AND OPERATION OF THE ROBOT

2.1. DESCRIPTION OF THE ROBOT

The positioning robot shown in Fig. 1 is an important part of the minimally invasive vascular interventional surgical robot system. The positioning robot consists of a base, an electric lifting pole and a five degrees-of-freedom (DOF) manipulator which includes a shoulder joint, an elbow joint, a wrist joint, an upper arm and a lower arm. Some parameters of the robot are shown in Table 1. The end-effector is fixed on the end of the positioning robot and a six-dimensional force sensor is fixed on the end-effector. By controlling the angle of each joint, the end-effector can be positioned in the best working position.

Table 1

Parameters of the robot

Joint	Power(w)	Maximal torque (Nm)	Maximal speed (deg./s)	Angle range (deg.)
Shoulder joint rotation	150	15.47	152.3	–80–170
Shoulder joint flexion	150	26.52	129.2	–90–90
Elbow joint flexion	150	26.52	208.2	–90–90
Wrist joint rotation	22	2.69	460.8	–135–115
Wrist joint flexion	22	3.55	216.7	–90–90

2.2. CALIBRATION OF THE ROBOT

Calibration of robot needs a space bigger than robot workspace, but there is not enough space to calibrate the robot in the surgery scene. To avoid the position calibration with large range motion before operating, three absolute position encoders are installed in shoulder joint rotation, shoulder joint flexion and elbow joint rotation shown in Fig. 2. To reduce the weight of moving parts of the robot and realize the compact design of the three joints, three absolute encoders are located at end of the robot and the angles of the three joints are measured by rope drive. The absolute position encoder is determined by the mechanism position of the photoelectric encoder and the information of its position can be remembered after power off. So the position of robot can be known after power on and the calibration of those three joints is unnecessary. In this way, the calibration time can be saved to improve the efficiency.
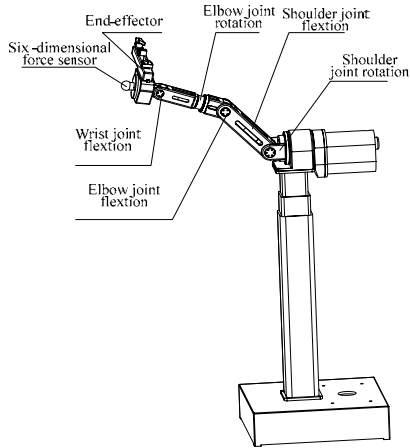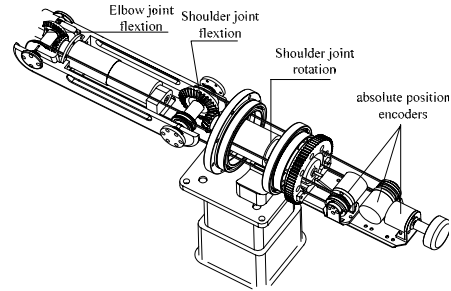
Fig. 1 – The positioning robot.   Fig. 2 – Structure drawing.

2.3. MANIPULATION OF THE ROBOT

A six-dimensional force sensor developed by the Yanshan University research team is fixed on the end of the robot. The operator can operate this force sensor to adjust the position and orientation of the robot at any moment. This way of operation can effectively avoid the settled programmable control mode and it is an user-friendly operation way in line.
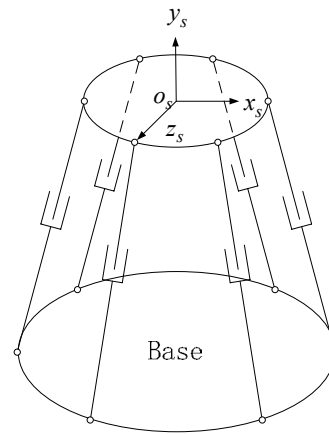

Fig. 3 – The six-dimensional force sensor.   Fig. 4 – Stewart platform.

The six-dimensional force sensor (shown in Fig. 3) is a strain sensor. The elastomer of the sensor is a Stewart parallel mechanism (shown in Fig. 4). Its spatial coordinate is set up on the moving platform and the origin is the center of

the platform. The six-dimensional force and moment imposed on the sensor by the operator can be transferred into the elastic deformation of the six poles in the sensor, and the elastic deformation can be measured by the strain gauge pasted on each pole. The conversion between strain and voltage signal can be realized by full bridge circuit, and the six-dimensional voltage signals are output by USB communication.

3. ANALYSIS OF MANIPULATION MODE

3.1. FORCE SIGNAL TRANSFORM

We directly use the six-dimensional voltage signals outputted to control the positioning robot. From the six-dimensional voltage $\mathbf{L}_v = \begin{bmatrix} L_{v1} & L_{v2} & \cdots & L_{v6} \end{bmatrix}^{\mathrm{T}}$, the six-dimensional force can be obtained as follows

$$\mathbf{F} = \begin{bmatrix} G \end{bmatrix}\mathbf{L}_v, \tag{1}$$

where $[G]$ is a calibration matrix of the force sensor [20]. $\mathbf{F} = \begin{bmatrix} F_x & F_y & F_z & M_x & M_y & M_z \end{bmatrix}^{\mathrm{T}}$ is a six-dimensional force signals outputted from the sensor.

3.2. THE END POSITION OF THE ROBOT

According to the work principle of the six-dimensional sensor, it can be seen that the displacement of the robot is proportional to the magnitude of the corresponding force. So the displacement along a certain direction can be figured out by multiplying a coefficient $K_f > 0$ based on the component of the force.

$$\mathbf{P}_i = K_f \mathbf{F}_i \ \ (i = x, y, z). \tag{2}$$

The equivalent vector $\mathbf{k}'$ of the moment components can be obtained as follows

$$\mathbf{k}' = M_x \mathbf{i} + M_y \mathbf{j} + M_z \mathbf{k}, \tag{3}$$

The unit vector $\mathbf{k}$ corresponding to the vector $\mathbf{k}'$ is calculated as follows

$$\mathbf{k} = \mathbf{k}' / |\mathbf{M}|, \tag{4}$$

where

$$|\mathbf{M}| = \sqrt{M_x{}^2 + M_y{}^2 + M_z{}^2} \ .$$

The projections of the unit vector onto the three axes are

$$\begin{cases} K_x = M_x / |\mathbf{M}| \\ K_y = M_y / |\mathbf{M}| \\ K_z = M_z / |\mathbf{M}| \end{cases} \tag{5}$$

According to the work principle of the six-dimensional sensor, it can be seen that the attitude change of the positioning robot is proportional to the magnitude of the corresponding moment. And the rotating angle around a certain axis can be figured out by multiplying a coefficient $K_m > 0$ based on the module of the moment. So the rotation angle θ around the vector $\mathbf{k}$ is

$$\theta = K_m |\mathbf{M}| . \tag{6}$$

The target position and orientation matrix T_s of the positioning robot can be expressed as follows

$$T_s = \begin{bmatrix} N_{xs} & O_{xs} & A_{xs} & P_{xs} \\ N_{ys} & O_{ys} & A_{ys} & P_{ys} \\ N_{zs} & O_{zs} & A_{zs} & P_{zs} \\ 0 & 0 & 0 & 1 \end{bmatrix} \tag{7}$$

This expression is based on the coordination of the sensor. In order to make the calculation more conveniently, the matrix T_s should be transformed into the coordination of the positioning robot first. The target position and orientation matrix T_a in the coordination of the positioning robot can be obtained in the following equation

$$T_a = T_s \, {}_a^s T . \tag{8}$$

To control the movement of the positioning robot, its position and orientation have to be calculated. According to the size and construction of the designed machine, the transfer matrix ${}_a^s T$ can be expressed as follow

$${}_a^s T = \text{Trans}(y, -130)\text{Rot}(x, 90°)\text{Rot}(z, -90°) = \begin{bmatrix} 0 & 1 & 0 & 0 \\ 0 & 0 & -1 & -130 \\ -1 & 0 & 0 & 0 \\ 0 & 0 & 0 & 1 \end{bmatrix} . \tag{9}$$

The end position matrix T_a of the robot can be expressed as

$$T_a = \begin{bmatrix} N_{xa} & O_{xa} & A_{xa} & P_{xa} \\ N_{ya} & O_{ya} & A_{ya} & P_{ya} \\ N_{za} & O_{za} & A_{za} & P_{za} \\ 0 & 0 & 0 & 1 \end{bmatrix} = \begin{bmatrix} -A_{xs} & N_{xs} & -O_{xs} & -130A_{xs} + P_{xs} \\ -A_{ys} & N_{ys} & -O_{ys} & -130A_{ys} + P_{ys} \\ -A_{zs} & N_{zs} & -O_{zs} & -130A_{zs} + P_{zs} \\ 0 & 0 & 0 & 1 \end{bmatrix} , \tag{10}$$

where

$$N_{xa} = -K_z K_x (1-\cos\theta) - K_y \sin\theta \qquad\qquad N_{ya} = -K_z K_y (1-\cos\theta) - \cos\theta$$

$$N_{za} = -K_z K_z (1-\cos\theta) - \cos\theta \qquad\qquad O_{xa} = K_x K_x (1-\cos\theta) + \cos\theta$$

$$O_{ya} = K_y K_x (1-\cos\theta) + K_z \sin\theta \qquad\qquad O_{za} = K_z K_x (1-\cos\theta) - K_y \sin\theta$$

$$A_{xa} = -K_y K_x (1-\cos\theta) + K_z \sin\theta \qquad\qquad A_{ya} = -K_y K_y (1-\cos\theta) - \cos\theta$$

$$A_{za} = -K_z K_y (1-\cos\theta) - K_x \sin\theta \qquad P_{xa} = 130\left(K_y K_x (1-\cos\theta) - K_z \sin\theta\right) + K_f F_x$$

$$P_{ya} = 130\left(K_y K_y (1-\cos\theta) + \cos\theta\right) + K_f F_y \quad P_{za} = 130\left(K_z K_y (1-\cos\theta) + K_x \sin\theta\right) + K_f F_z.$$

The target matrix can be known after the coefficient K_x, K_y, K_z, K_f being obtained. Make the target matrix as the end position and orientation of the positioning robot, and calculate inverse kinematics to change the every target matrixes into the joint angles. By fitting a smooth function to every joint and making the joint rotation following the corresponding functions, the positioning robot will pass all point of the path to reach the target position.

As an easy example, suppose that $K_x = 1$, $K_y = 1$, $K_z = 1$, $K_f = 10$ mm/N , and then impose a 15N force on the sensor along its Z axis. That is $|M| = 0$, $F_x = 0$, $F_y = 0$, $F_z = 15$ N . Substituting these values into formula (10), we can be easily obtained that only the value of P_{za} is increased 150 mm and other positions and orientations are not changed. That is to say, under the action of the 15 N force, the robot moves 150 mm along the Z axis.

3.3. KINEMATICS ANALYSIS

Since the positioning robot has five-DOF and the target matrix is obtained by a six-DOF manipulator, we couldn't make sure that the positioning robot can reach every position given by the matrix. Therefore, a fictitious joint is added to make the robot become a full freedom manipulator. The added fictitious joint is perpendicular to the two end joints and passes the intersecting point of the two end joint axis [30, 31]. In this way, the problem of solving the inverse kinematics of the five-DOF manipulator can be translated into that of the six-DOF manipulator. The above matrix (10) translated by six dimensional force signals can be taken as the end position and orientation of the six-DOF manipulator. Then the inverse kinematics of this mechanism can be calculated. Locking the fictitious joint, the other five variables of the joints have been expressed. According to these expressions, we can further do trajectory planning to realize compliance control to the positioning robot by operating a six-dimensional force sensor.

3.3.1. Forward kinematics of the five-DOF manipulator

Depending on the D-H method, the coordinate system of every joint for the positioning robot can be established. The diagram of the initial position of the
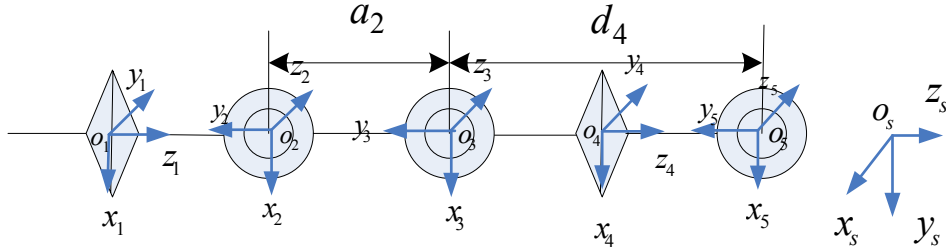
positioning robot is shown in Fig. 5.

Fig. 5 – Structure diagram of the five-DOF manipulator.

The robot position and orientation matrix can be obtained as follows

$$
{}^{0}_{5}T = \prod_{i=1}^{5} {}^{i-1}_{i}T = {}^{0}_{1}T \, {}^{1}_{2}T \, {}^{2}_{3}T \, {}^{3}_{4}T \, {}^{4}_{5}T \, . \tag{11}
$$

3.3.2. Forward kinematics of six-dof manipulator

According to the diagram in Fig. 3, the Plücker coordinates of the motion vector in the base coordinate are

$$\$_1=(0\ 0\ 1,\ 0\ 0\ 0);\ \ \$_2=(0\ 1\ 0,\ 0\ 0\ 0);\ \ \$_3=(0\ 1\ 0,\ a_2\ 0\ 0);$$
$$\$_4=(0\ 0\ 1,\ a_2\ 0\ d_4);\ \ \$_5=(0\ 1\ 0,\ a_2\ 0\ d_4).$$

The anti-spiral of the screw system is

$$\$_r= (1\ 0\ 0,\ 0\ k\ 0). \tag{12}$$

From the above screw (12), it can be seen there is a constraint along the direction of the X axis of the base coordinate system. Adding one degree of freedom along this direction and removing the constraint, the structure diagram of the six-DOF manipulator shown in Fig. 6 can be obtained.
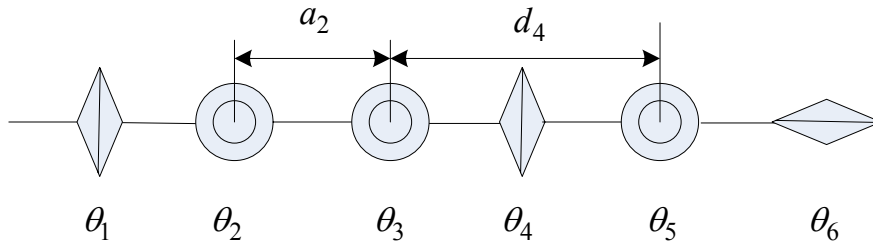

Fig. 6 – Structure diagram of the six-DOF manipulator.

The freedom added only changes the orientation of the robot. It is an independent freedom and it is not influenced by the other five-DOF. From the six-DOF robot, the solution equations of the first five variables which are the inverse solution of the five-DOF manipulator can be obtained.

The position and orientation matrix of six-DOF manipulator is

$$
{}_6^0T = \prod_{i=1}^{6} {}_i^{i-1}T = {}_1^0T\,{}_2^1T\,{}_3^2T\,{}_4^3T\,{}_5^4T\,{}_6^5T = \begin{bmatrix} n_x & o_x & a_x & p_x \\ n_y & o_y & a_y & p_y \\ n_z & o_z & a_z & p_z \\ 0 & 0 & 0 & 1 \end{bmatrix}. \tag{13}
$$

3.3.3. Inverse kinematics

Setting ${}_6^0T$ equals to the matrix T_a, the inverse kinematics of the six-DOF manipulator can be resolved. According to the analysis above, the solutions of the first five angles can be expressed as

$$
\theta_1 = \arctan\left(p_y / p_x\right),
$$

$$
\theta_2 = 2\arctan(t), \quad t = \left(-b \pm \sqrt{b^2 - 4ac}\right)\Big/(2a),
$$

$$
\theta_3 = \arccos\left(\left(c_1 s_2 p_x + s_1 s_2 p_y + c_2 p_z\right)\Big/(d_4)\right), \tag{14}
$$

$$
\theta_5 = \arccos\left(a_z c_{23} \pm \sqrt{a_z^2 c_{23} - 4\left(a_z^2 + \left(\left(s_1 a_x - c_1 a_y\right)^2 - 1\right)s_{23}^2\right)}\right),
$$

$$
\theta_4 = \arcsin\left(\left(s_1 a_x - c_1 a_y\right)\Big/s_5\right),
$$

where

$$
a = c_1^2 p_x^2 + s_1^2 p_y^2 + p_z^2 + a_2^2 - d_4^2 + 2s_1 c_1 p_x p_y + 2c_1 p_x a_2 + 2s_1 p_y a_2
$$

$$
b = 4 p_z a_2
$$

$$
c = c_1^2 p_x^2 + s_1^2 p_y^2 + p_z^2 + a_2^2 - d_4^2 + 2s_1 c_1 p_x p_y - 2c_1 p_x a_2 - 2s_1 p_y a_2 \, .
$$

From the above analysis and calculation, the signals of the six-dimensional force sensor can been translated into the rotational angles of each joint. Therefore, the compliance control of the manipulator can be realized by operating the six-dimensional force sensor.

4. EXPERIMENT

The experiment is conducted to verification the proposed method. The experimental platform is shown in Fig. 7. By operating the six-dimensional force sensor a certain distance along the horizontal direction, the five joint angle curves can be obtained as shown in Fig. 8. Making those curves as the inputs of the five-DOF positioning robot and substituting them into the forward kinematics equations of the robot, we can obtain a motion curve. Constructing this curve with the pre-set line, the correction of the analysis in section 3 is verified. From Fig. 9, it can be noticed that the error between the factual trace (the dashed line) and the pre-set line (the real line) is small.
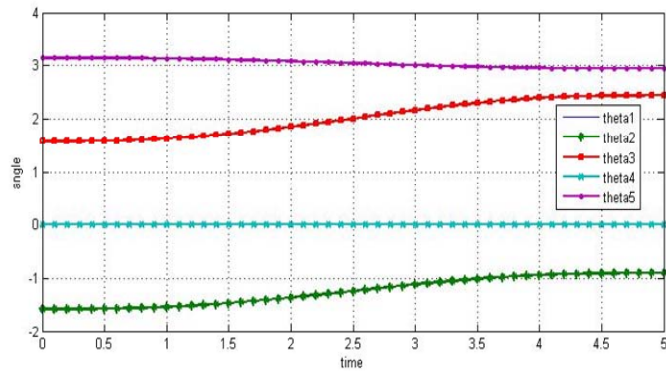

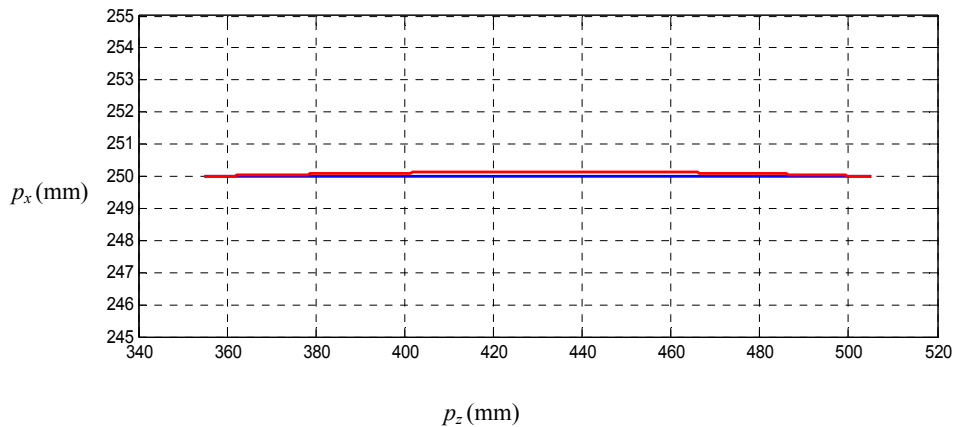Fig. 7 – Experimental platform.

Fig. 8 – Angle change curves.

Fig. 9 – Experimental result.

5. CONCLUSION

This paper has proposed the calibration and operation modes of a positioning robot used for minimally invasive vascular interventional surgery.

Three absolute position encoders are installed in the shoulder, elbow and wrist joints, respectively, which can avoid the position calibration of the shoulder joint rotation, shoulder joint flexion and elbow joint rotation with large range motion before operating. The position of robot can be known after power on and the calibration of those three joints is unnecessary. In this way, the calibration time can be saved to improve the efficiency.

By dragging a force sensor fixed on the positioning robot, the position and orientation of the robot can be adjusted at any moment. This way of operation can effectively avoid the settled programmable control mode and it is a user-friendly operation way in line.

Finally, an experiment is given to verify whether the mode of calibration and operation is effective. The experimental results have demonstrated that the proposed method is effective, safe, and reliable and has a potential application. The mechanism developed in this paper provides a good supporting case for the HAM framework.

REFERENCES

1. H. Yu. *Overview of Human Adaptive Mechatronics*, Proceedings of the 9th WSEAS International Conference on Mathematics and Computers in Business and Economics, Bucharest, Romania, **20**, *4*, pp. 152–157, June, 2008.
2. W. S. Lu, D. Liu, Z. M. Tian and D. P. Zhang, *The Analysis of Key Technologies of Intravascular Intervention Surgical Robot*, Journal of Biomedical Engineering Research, **28**, *4*, pp. 303–306, 2009.
3. Z. C. Zheng, W. P. Yang and X. H. Chen, *The Application of DSA in Intervention Surgery*, Journal of Youjiang Medical College for Nationalities, **31**, *4*, pp. 683–684, 2009.
4. B. F. Zeng. *Minimally Invasive Surgery in Fracture Management*, Chinese Medical, **121**, *15*, pp. 1349–1351, 2008.
5. J. A. Zhang, L. M. Lin and G. M. Wang, *The Recent Study and Key Technologies of an Aided Endoscopic Surgical Robot System*, Chinese Journal of Medical Instrumentation, **26**, *1*, pp. 54–58, 2002.
6. Z. J. Du, L. N. Sun and L. X. Fu, *Development and Perspective of Robot Assisted Surgery*, High Technology Letters, **13**, *6*, pp. 106–110, 2003.
7. H. M. Garcia-Garcia, K. Tsuchida, H. Meulenbrug, A. T. Ong, J. Van der Giessen and P.W. Serruys, *Magnetic Navigation in a Coronary Phantom: Experimental Results*. Eurointervention, **1**, *3*, pp. 321–328, 2005.

8. D. Steve, H. Servatius, T. Rostock, B. Hoffmann, I. Drewitz, K. Müllerleile, A. Sultan, M. A. Aydin, T. Meinertz and S. Willems, *Reduced Fluoroscopy During Atrial Fibrillation Ablation: Benefits of Robotic Guided Navigation*, Cardiovasc Electrophysiol, **21**, *1*, pp. 6–12, 2010.

9. L. Di Biase, Y. Wang, R. Horton, G. J. Gallinghouse, P. Mohanty, J. Sanchez, D. Patel, M. Dare, R. Canby, L. D. Price, J. D. Zagrodzky, S. Bailey, J. D. Burkhardt and A. Natale, *Ablation of Atrial Fibrillation Utilizing Robotic Catheter Navigation in Comparison to Manual Navigation and Ablation: Single-center Experience*, Cardiovasc Electrophysiol, **20**, *12*, pp. 1328–1335, 2009.

10. R. Beyar, T. Wenderow, D. Lindner, G. Kumar and R. Shofti, *Concept, Design and Pre-clinical Studies for Remote Control Percutaneous Coronary Interventions*, EuroIntervention, **1**, *3*, pp. 340–345, 2005.

11. R. Beyar, L. Gruberg, D. Delleanu, A. Roguin, Y. Almagor, S. Cohen, G. Kumar, and T. Wenderow, *Remote-control Percutaneous Coronary Interventions. Concept, Validation, and First-in-humans Clinical Trial*, Journal of the American College of Cardiology, **47**, *2*, pp. 296–300, 2006.

12. S. B. Solomon, A. Patriciu, M. E. Bohlman, L. R. Kavoussi and D. Stoianovici, *Robotically Driven Interventions: a Method of Using CT Fluoroscopy without Radiation Exposure to the Physician*, Radiology, **225**, *1*, pp. 277–282, 2002.

13. J. Marescaux, J. Leroy, M. Gagner, *Transatlantic Robot-assisted Telesurgery*, Nature, **413**, *6854*, pp. 379–380, 2001.

14. M. Argenziano, M. Katz, J. Bonatti, J. Bonatti, S. Srivastava, D. Murphy, R. Poirier, D. Loulmet, L. Siwek, U. Kreaden and D. Ligon, *Results of the Prospective Multicenter Trial of Robotically Assisted Totally Endoscopic Coronary Artery Bypass Grafting*, Ann Thorac Surg., **81**, *5*, pp. 1666–1674, 2006.

15. V. A. Subramanian, N. U. Patel, N. C. Patel and D. F. Loulmet, *Robotic Assisted Multivessel Minimally Invasive Direct Coronary Artery Bypass with Port-access Stabilization and Cardiac Positioning: Paving the Way for Outpatient Coronary Surgery?*, Ann Thorac Surg., **79**, pp. 1590–1596, 2005.

16. D. S. Kwon, Y. S. Yoon, J. J. Lee, S. Y. Ko, K. H. Huh, *et al.*, *THROBOT: a New Surgical Robot System for Total Hip Arthroplasty*, 2001 IEEE/RSJ International Conference on Intelligent Robots and Systems, **2**, pp. 1123–1128, 2001.

17. H. Y. Kim, D. A. Streit, *Configuration Dependent Stiffness of the PUMA 560 Manipulator: Analytical and Experimental Results*, Mechanism and Machine Theory, **30**, *8*, pp. 1269–1277, 1995.

18. S. J. Harris, F. Arambula-Cosio, Q. Mei, R. D. Hibberd, *et al.*, *Probot – an Active Robot for Prostate Resection*, Proceedings of the Institution of Mechanical Engineers, Part H: Journal of Engineering in Medicine, **211**, *4*, pp. 317–325, 1997.

19. P. Joanne. *ROBODOC – Surgical Robot Success Story*, Industrial Robot: An International Journal, **24**, *3*, pp. 231–233, 1997.

20. J. Bergsland, E. Mujanovic, O. J. Elle, P. Mirtaheri, E. Fosse, *Robotic Manipulators in Cardiac Surgery: the Computer-assisted Surgical System ZEUS*, Minim Invasive Therapy Allied Technology, **10**, *6*, pp. 275–281, 2001.

21. J. Marescaux, F. Rubino, *The ZEUS Robotic System: Experimental and Clinical Applications*, Surgical Clinics of North America, **83**, *6*, pp. 1305–1315, 2003.

22. T. Ortmaier, G. Hirzinger, *Cartesian Control Issues for Minimally Invasive Robot Surgery*, IEEE International Conference on Intelligent Robots and Systems, **1**, pp. 565–571, 2000.

23. Y. Bailly, A. Chauvin, Y. Amirat, *Control of a High Dexterity Micro-robot Based Catheter for Aortic Aneurysm Treatment*, 2004 IEEE Conference on Robotics, Automation and Mechatronics, 2004, pp. 65–70.

24. K. Y. Kim, H. S. Song, J. J. Lee, *Control of a High Dexterity Micro-robot Based Catheter for Aortic Aneurysm Treatment*, Proceedings of the 2008 International Conference on Bioinformatics and Computational Biology, BIOCOMP, 2008, pp. 977–983.
25. K. Y. Kim, H. S. Song, J. W. Suh, J. J. Lee, *Human Arm-like Surgical Robot System with Force Reflection Measurement for Minimally Invasive Surgery*, Proceedings of the 14th International Symposium on Artificial Life and Robotics, (AROB), **14**, pp. 313–316, 2009.
26. G. Paula, Surgical Robotics: *Reviewing the Past, Analyzing the Present, Imagining the Future*, Robotics and Computer-Integrated Manufacturing, **27**, pp. 261–266, 2011.
27. I. Kamran, L. B. David, *Robotic Liver Surgery*, Surgical Clinics of North America, **90**, *4*, pp. 761–774, 2010.
28. B. Franck, *Indications and the Role of Laparoscopic Partial Nephrectomy*, European Urology Supplements, **9**, *3*, pp. 454–458, 2010.
29. M. P. Young, S. K. Won, K. B. Hyung, D. V. Armando, S. J. Jin, K. Se-Heon, *Feasibility of Transoral Robotic Hypopharyngectomy for Early-Stage Hypopharyngeal Carcinoma*, Oral Oncology, **46**, *8*, pp. 597–602, 2010.
30. M. Rachid, L. D. Keith, *A Complete Kinematics of Four-Revolute-Axis Robot Manipulators*, Mech. Mach. Theory., **27**, *5*, pp. 575–586, 1992.
31. M. Rachid, L. D. Keith, *Fast Inverse Kinematics of Five-Revolute-Axis Robot Manipulators*, Mech. Mach. Theory, **27**, *5*, pp. 587–597, 1992.